Rapid Flip-Flop of Phospholipids in Endoplasmic Reticulum Membranes Studied by a Stopped-Flow Approach

Uwe Marx,* Günter Lassmann,† Hermann-Georg Holzhütter,‡ Daniel Wüstner,* Peter Müller,* Astrid Höhlig,* Janek Kubelt,* and Andreas Herrmann*

*Humboldt-Universität zu Berlin, Mathematisch-Naturwissenschaftliche Fakultät I, Institut für Biologie/Biophysik, D-10115 Berlin, †Technische Universität Berlin, Max-Volmer-Institut für Biophysikalische Chemie und Biochemie, D-10623 Berlin, and ‡Humboldt-Universität zu Berlin, Charite, Bereich Medizin, Institut für Biochemie, D-10117 Berlin, Germany

ABSTRACT The transbilayer movement of short-chain spin-labeled and fluorescent 7-nitrobenz-2-oxa-1,3-diazol-4-yl (NBD) phospholipid analogs in rat liver microsomes is measured by stopped-flow mixing of labeled microsomes with bovine serum albumin (BSA) solution. Extraction of analogs from the outer leaflet of microsomes to BSA can be directly monitored in conjunction with electron paramagnetic resonance or fluorescence spectroscopy by taking advantage of the fact that the signal of spin-labeled or fluorescent analogs bound to BSA is different from that of the analogs inserted into membranes. From the signal kinetics, the transbilayer movement and the distribution of analogs in microsomal membranes can be derived provided the extraction of analogs by BSA is much faster in comparison to the transbilayer movement of analogs. Half-times of the back-exchange for spin-labeled and fluorescent analogs were <3.5 and <9.5 s, respectively. The unprecedented time resolution of the assay revealed that the transbilayer movement of spin-labeled analogs is much faster than previously reported. The half-time of the movement was about 16 s or even less at room temperature. Transmembrane movement of NBD-labeled analogs was six- to eightfold slower than that of spin-labeled analogs.

INTRODUCTION

The ER is the major site of phospholipid biosynthesis and thus plays a central role in the biogenesis of its own phospholipid bilayer and that of the other cellular membranes. The active sites of the phospholipid-synthesizing enzymes, such as e.g., the PC-synthesizing enzyme CDP-choline, 1,2-diacylglycerol phosphocholine transferase, are located on the cytoplasmic leaflet of the ER. Consequently, phospholipids synthesized by these enzymes first appear on the cytosolic face of the ER. To preserve membrane stability and genesis, efficient mechanisms must be available to move newly synthesized phospholipids to the lumenal face of the ER. Indeed, for various types of labeled phospholipid analogs, a redistribution to the lumenal leaflet of the rat liver ER membrane and vice versa has been shown (Bishop and Bell, 1985; Baker and Dawidowicz, 1987; Herrmann et al., 1990; Buton et al., 1996; Berr et al., 1993). Recently, Buton et al. (1996) reported a half-time of ~30 s for bidirectional transbilayer movement of short-chain spin-labeled phospholipids in rat liver microsomal membranes. The results of Buton et al. (1996) and others (Bishop and Bell, 1985; Baker and Dawidowicz, 1987; Herrmann et al., 1990) strongly indicate that lipid-transporting membrane proteins, so-called "flippases," are involved in phospholipid transbilayer movement in the ER.

However, due to the comparatively low time resolution of available assays, transbilayer phospholipid dynamics may be difficult to quantify and, thus, might be underestimated. Typically, phospholipid analogs with a short chain in the *sn*-2 position bearing either a paramagnetic nitroxide moiety or a fluorescent group such as NBD are used. Commonly, redistribution of those analogs across membranes is followed by the selective extraction of analogs by BSA from the outer leaflet that is accessible to BSA, the so-called back-exchange assay (Haest et al., 1981; Morrot et al., 1989; Herrmann et al., 1990; Connor et al., 1990; Colleau et al., 1991; Fellmann et al., 1994). To distinguish between analogs accessible to BSA and those residing on the inner leaflet, a centrifugation step is required to separate membranes from the suspension medium containing BSA/analog complexes. Despite considerable improvement (Buton et al., 1996), this centrifugation step limits the resolution for detecting kinetics of rapid transbilayer lipid redistribution. Indeed, Buton et al. (1996) already pointed out that their translocation assay with a time resolution of ~30 s may only allow definition of an upper limit for the half-time of phospholipid transbilayer movement in rat liver microsomal membranes.

Received for publication 15 November 1999 and in final form 28 February 2000.

Address reprint requests to Andreas Herrmann, Humboldt-Universität zu Berlin, Mathematisch-Naturwissenschaftliche Fakultät I, Institut für Biologie/Biophysik Invalidenstrasse 42, D-10115 Berlin, Germany. Tel: +49-30-20938830; Fax: +49-30-20938585; E-mail: Andreas=Herrmann@rz.hu-berlin.de.

Abbreviations used: ER, endoplasmic reticulum; BSA, bovine serum albumin; CDP, cytidine diphosphate; DFP, diisopropyl fluorophosphate; EPR, electron paramagnetic resonance; MB, microsome buffer; NBD, 7-nitrobenz-2-oxa-1,3-diazol-4-yl; N-Rh-PE, L-α-phosphatidylethanolamine-*N*-(lissamine rhodamine B sulfonyl)(egg); PC, phosphatidylcholine; P-C6-NBD-PC, 1-palmitoyl-2-[6-[(7-nitrobenz-2-oxa-1,3-diazol-4-yl)amino]caproyl]-*sn*-glycero-3-phosphocholine; P-C6-NBD-PE, 1-palmitoyl-2-[6-[(7-nitrobenz-2-oxa-1,3-diazol-4-yl)amino]caproyl]-*sn*-glycero-3-phosphoethanolamine; PE, phosphatidylethanolamine; POPC, 1-palmitoyl-2-oleoyl-*sn*-glycero-3-phosphocholine; SL-PC, 1-palmitoyl-2-(4-doxylpentanoyl)-*sn*-glycero-3-phosphocholine; SL-PE, 1-palmitoyl-2-(4-doxylpentanoyl)-*sn*-glycero-3-phosphoethanolamine.

0006-3495/00/05/2628/13 $2.00

In the present study, we have developed a stopped-flow assay that provides a sufficiently high resolution for the characterization of rapid lipid transbilayer movement in ER and other membranes. We have measured the transbilayer distribution and movement of NBD- and spin-labeled short-chain analogs in rat liver microsomal membranes by this assay, which is also based on selective extraction of membrane-incorporated analogs "back" to the acceptor BSA. However, the major improvement is to make use of the fact that the signal of both spin-labeled and fluorescent analogs bound to BSA is different from that of the analogs incorporated into membranes. Thus, extraction can be followed quantitatively even in the presence of BSA. By that, the formerly obligatory centrifugation step for separation is no longer required. Thus, using fluorescence or EPR spectroscopy in conjunction with stopped-flow mixing, our approach allows monitoring of transbilayer distribution and movement of analogs in real time (i.e. on-line) with a high time resolution. Resolving lipid transbilayer movement is only limited by the rate constant of analog exchange to BSA. We found that previous studies indeed underestimated the transbilayer dynamics of phospholipid analogs across ER membranes. Short-chain spin-labeled phospholipid analogs redistribute nearly symmetrically between both leaflets of rat liver microsomes with a half-time of about 16 s or even less at room temperature. Although transbilayer distribution of NBD-labeled analogs was also nearly symmetrical, the transverse movement was six- to eightfold slower, pointing to a substantial influence of the NBD moiety on lipid dynamics. The stopped-flow back-exchange assay provides a suitable tool for the identification of flippases either by reconstitution or by screening for mutants with defects in lipid translocation across the ER membrane.

MATERIALS AND METHODS

Materials

POPC was obtained from Sigma-Aldrich Chemie GmbH (Deisenhofen, Germany). *N*-Rh-PE, P-C6-NBD-PC, and P-C6-NBD-PE were from Avanti Polar Lipids (Alabaster, AL, USA). SL-PC and SL-PE were synthesized as described (Fellmann et al., 1994). All other chemicals and reagents were from Sigma-Aldrich Chemie GmbH.

Preparation of smooth rat liver microsomes

Smooth rat liver microsomes were prepared according to the method developed by Tauber et al. (1986). A fresh rat liver (weight ~8–10 g) was finely scissor-minced and homogenized with a Servodyne homogenizer (Heidolph-Elektro GmbH, Kelheim, Germany) in ice-cold 100 mM Tris-HCl buffer, pH 7.0 containing 10% (w/w) sucrose to yield a 25% (w/v) homogenate. The homogenate was centrifuged at 1000 × *g* for 15 min. All centrifugations were carried out at 4°C. The resulting supernatant was diluted with two volumes of liver medium (1 mM $NaHCO_3$, 0.5 mM $CaCl_2$) and centrifuged at 12,000 × *g* for 25 min (type 45 Ti rotor, Beckman Instruments Inc., Spinco Div., Palo Alto, CA, USA). The resulting pellet of crude ER membranes was resuspended in ice-cold 100 mM Tris-HCl buffer, pH 7.0, containing 34% (w/w) sucrose and was adjusted to a final concentration of 32% (w/w) sucrose. The crude ER membranes were applied to a gradient consisting of 1.5 ml 38% (w/w) sucrose, 1.5 ml 34% (w/w) sucrose, 1.5 ml 30% (w/w) sucrose, and 1.5 ml 10% (w/w) in 100 mM Tris-HCl buffer, pH 7.0. After centrifugation at 100,000 × *g* for two hours (SW 40 Ti rotor, Beckman Instruments), purified smooth microsomes were collected from the 34/38% sucrose interface, diluted with ice-cold buffer MB (50 mM Tris-HCl, pH 7.4, 0.25 M saccharose, 1 mM $MgSO_4$) and sedimented by centrifugation for one hour at 100,000 × *g* (SW 40 Ti rotor, Beckman Instruments). The smooth microsomal pellet was rehomogenized with a Potter-Elvejhem homogenizer in 5 ml ice-cold MB. Smooth microsomes contained 0.46 ± 0.04 mg phospholipid/mg protein. This value is very similar to the value of 0.37 mg phospholipid/mg protein reported by Daum (1985).

Steady-state measurements

All steady-state measurements were performed at room temperature. Steady-state EPR measurements were done using an X-band EPR spectrometer (type: ECS 106, BRUKER Analytische Messtechnik GmbH, Karlsruhe, Germany). Steady-state fluorescence measurements were done using an Aminco Bowman Series 2 spectrofluorometer (SLM Instruments Inc., Rochester, NY, USA).

Stopped-flow measurements

All stopped-flow measurements were performed at room temperature.

Stopped-flow EPR measurements

Stopped-flow EPR measurements were done using a commercially available EPR stopped-flow accessory (Center of Scientific Instruments of the former Academy of Sciences and Galenus GmbH, Berlin-Adlershof, Germany) attached to an X-band EPR spectrometer (type ERS 300 E, BRUKER Analytische Messtechnik GmbH) using the rectangular H_{102} resonator. The EPR cell is a thick-walled cylindrical quartz capillary of 1.3 mm inner diameter (sample volume: 30 μl) connected immediately with the mixer. One mixing shot needs 70 μl of each of the two liquid components that are stored in glass syringes (1.6 ml each). Stroking magnets drive the two components through the mixer and into the EPR cell. Behind the EPR cell, the flow is stopped by an electrically controlled stop-valve setting the trigger for recording a time-sweep (for further details and applications, see Lassmann et al., 1992; Marx et al., 1997). The mixing takes ~1 ms and the dead time (time between mixing and entering the EPR cell) another 1 ms. Although the stopping time is only 0.5 ms, the stop valve causes mechanical disturbances that impact the microwave detection system and last some milliseconds. The overall dead time of the apparatus has been measured to be ≤10 ms, that is, ≤10 ms after setting the trigger for recording a time-sweep, the EPR signal is free of any disturbance from the stopped-flow accessory.

Stopped-flow fluorescence measurements

Stopped-flow fluorescence measurements were accomplished using a commercially available stopped-flow device with a dead time of <10 ms (RX. 1000 Rapid Kinetics Spectrometer Accessory, Applied Photophysics, Leatherhead, UK) coupled to an Aminco Bowman Series 2 spectrofluorometer (SLM Instruments). One mixing shot needs 80 μl of each of the liquid components.

Incorporation of analogs into microsomal membranes

Spin-labeled analogs

SL-PC or SL-PE were resuspended in buffer MB and mixed with rat liver microsomal membranes in the EPR stopped-flow cell (final concentrations

of phospholipid analog and microsomal phospholipid were 0.1 and 2 mM, respectively). The kinetics of analog incorporation were followed by measuring the change of the EPR amplitude at a magnetic field position corresponding to the maximum of the high-field peak of the analog membrane spectrum (see Results and Marx et al., 1997). The specific parameters of EPR measurement were: conversion time, 20.48 ms; time constant, 5.12 ms. To improve the signal-to-noise ratio of the kinetics, the EPR spectrum was overmodulated with a modulation amplitude of 5 G.

NBD-labeled analogs

Stock solution of P-C6-NBD-PC or P-C6-NBD-PE, 1.5 ml 0.14 μM, was mixed with 500 μl rat liver microsomal membrane suspension (2 mM microsomal phospholipid; microsomal membrane suspension had been preincubated for 10 min with 5 mM DFP at 37°C) and the NBD fluorescence emission intensity (λ_{ex} = 470 nm; λ_{em} = 540 nm; width of slits, 4 nm; time trace scan resolution, 0.5 s) was monitored as a function of time.

Stopped-flow back-exchange assay

Spin-labeled analogs

Labeling of microsomes was performed by mixing freshly prepared rat liver microsomal membranes with SL-PC or SL-PE dispersed in aqueous buffer (final concentrations of phospholipid analog and microsomal phospholipid were 100 μM and 2 mM, respectively) and incubating for 5 min at room temperature. The time-dependent back-exchange of spin-labeled analogs from the microsomal membrane was monitored by mixing the labeled microsomes with an equal volume of 10% (w/v) BSA (final concentration) in the stopped-flow apparatus at room temperature. The time-dependent decrease of the EPR amplitude at a position corresponding to the maximum of the low-field peak of the membrane spectrum of the analogs reflects the kinetics of analog extraction (see Results). The specific parameters of EPR measurement were: conversion time, 81.92 ms; time constant, 20.48 ms. To improve the signal-to-noise ratio of the kinetics, the EPR spectrum was overmodulated with a modulation amplitude of 3 G.

NBD-labeled analogs

Before the experiments, freshly prepared rat liver microsomes were preincubated with 5 mM DFP for 10 min at 37°C. Labeling of microsomes was performed by mixing microsomal membranes with P-C6-NBD-PC or P-C6-NBD-PE dispersed in aqueous buffer (final concentrations of phospholipid analog and microsomal phospholipid were 0.4 μM and 1 mM, respectively) and incubating for 5 min (if not stated otherwise) at room temperature. The time-dependent back-exchange of NBD-labeled analogs from the microsomal membrane was monitored by mixing the labeled microsomes with an equal volume of 2% (w/v) BSA (final concentration) in the stopped-flow apparatus at room temperature. The time-dependent decrease of the NBD fluorescence emission intensity at 540 nm (λ_{ex} = 470 nm; width of slits, 4 nm; time trace scan resolution, 0.2 s) reflects the kinetics of analog extraction.

Preparation of *N*-Rh-PE-containing acceptor liposomes

Large unilamellar acceptor liposomes containing 3 mol% N-Rh-PE and 97 mol% POPC were prepared by the extrusion technique (Mayer et al., 1986). Briefly, 50 μl of a 0.02 M POPC stock solution in chloroform were mixed with 38 μl of a 0.8 mM *N*-Rh-PE stock solution in chloroform/methanol (9:1, v/v). The phospholipid mixture was dried under nitrogen and the phospholipids were resuspended in 1 ml of buffer MB by vortexing. The resulting aqueous phospholipid dispersion was subjected to five freeze–thaw cycles and was then extruded ten times through two 0.1-μm polycarbonate filters (Extruder was from Lipex Biomembranes Inc., Vancouver, Canada; filters were from Costar, Nucleopore GmbH, Tübingen, Germany).

Fluorescence resonance energy transfer-based assay

Before the experiments, freshly prepared rat liver microsomes were subjected to a 10-min preincubation with 5 mM DFP at 37°C. One hundred fifty microliters of the DFP-preincubated microsomes (1 mM phospholipid concentration) were injected into a cuvette containing 2 ml 0.24 μM stock solution of P-C6-NBD-PE in buffer MB. After 5 min incubation at room temperature, 200 μl of the *N*-Rh-PE-containing acceptor liposomes (97 mol% POPC, 3 mol% N-Rh-PE) were added. After addition of the acceptor liposomes, the NBD fluorescence emission intensity (λ_{ex} = 470 nm; λ_{em} = 540 nm; width of slits, 4 nm; time trace scan resolution, 0.5 s) was recorded as a function of time at room temperature.

Kinetic analysis

Estimation of rate constants for phospholipid transbilayer movement and for back-exchange to BSA was based on fitting the experimental data to theoretical time-courses computed on the basis of a three-compartment model (details are given in Results and Appendix). Fitting was performed by least-square minimization using the SOLVER-function of Microsoft EXCEL.

RESULTS

Incorporation of NBD- and spin-labeled analogs into rat liver microsomal membranes

Upon dispersion in aqueous buffer, NBD-labeled phospholipid analogs form micelles (Nichols, 1985). In such micelles, the fluorescence of the analogs is almost entirely self-quenched. Transfer of analogs from micelles to rat liver microsomal membranes is accompanied by a relief of self-quenching due to dilution of analogs by an excess of membrane lipids. The fluorescence increase can be directly monitored as a function of time (Fig. 1). As can be seen from Fig. 1, both P-C6-NBD-PC and P-C6-NBD-PE incorporate readily into rat liver microsomal membranes. About 90% of the analogs have incorporated into the microsomal membrane within 100 s at room temperature.

Dispersion of spin-labeled analogs in aqueous buffer likewise causes formation of micelles (King and Marsh, 1987). Due to the strong spin–spin interaction in micelles, a broad EPR spectrum is observed that is superimposed on a sharp spectrum with three narrow lines corresponding to monomers in suspension (see spectrum A in the inset in Fig. 2). Incorporation of aqueous dispersed spin-labeled analogs into microsomal membranes leads to a significant change in spectral line shape typical for a membrane spectrum (see spectrum B in the inset in Figure 2). By monitoring the amplitude of the high-field peak (see marking line in the inset in Figure 2), which is a sensitive measure of the spectral line shape, we were able to follow membrane

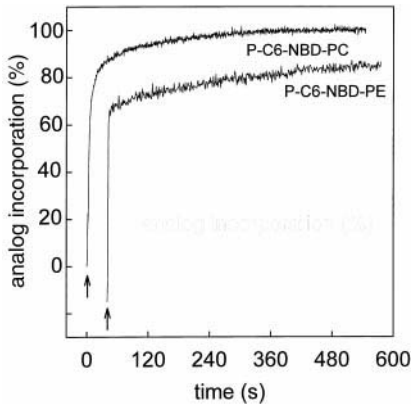

FIGURE 1 Kinetics of incorporation of NBD-labeled analogs into rat liver microsomal membranes. P-C6-NBD-PC and P-C6-NBD-PE were added to rat liver microsomes in buffer MB (final concentrations of NBD-labeled analogs and microsomal phospholipid were 0.1 μM and 0.5 mM, respectively) and the kinetics of membrane incorporation of the analogs were followed as described in Materials and Methods. The incorporation kinetics of P-C6-NBD-PE is displaced for clarity. The arrowhead indicates the time at which NBD-labeled analogs were mixed with the rat liver microsomes. The value of 100% corresponds to incorporation of all analogs. All experiments were performed at room temperature.

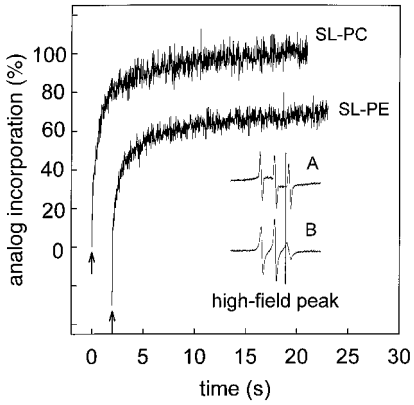

FIGURE 2 Kinetics of incorporation of spin-labeled analogs into rat liver microsomal membranes. SL-PC or SL-PE were added to rat liver microsomes in buffer MB (final concentrations of spin-labeled analogs and microsomal phospholipid were 0.1 and 2 mM, respectively) and the kinetics of membrane incorporation of the analogs were followed by means of stopped-flow EPR spectroscopy as described in Materials and Methods (specific parameters of EPR measurement: conversion time, 20.48 ms; time constant, 5.12 ms; modulation amplitude, 5 G). The incorporation kinetics for SL-PE is displaced for clarity. The arrowhead indicates the time at which spin-labeled analogs were mixed with the rat liver microsomes. (*Inset*) EPR spectrum of SL-PC dispersed in (*A*) aqueous buffer or (*B*) incorporated into rat liver microsomal membranes. The specific parameters for measurement of EPR spectra were: conversion time, 81.92 ms; time constant, 20.48 ms; modulation amplitude, 2 G; sweep width, 100 G. Kinetics were measured at the position of the high-field peak of spectrum B. The value of 100% corresponds to incorporation of all analogs. All experiments were performed at room temperature.

insertion of SL-PC and SL-PE as a function of time by the stopped-flow EPR technique. Spin-labeled analogs incorporate faster into rat liver microsomal membranes than the corresponding NBD-labeled analogs. Within 5 s at room temperature, 90% of the spin-labeled analogs have incorporated into the microsomal membrane. This value is similar to those reported previously by us for insertion of spin-labeled analogs into vesicle membranes of egg-PC and into erythrocyte membranes (Marx et al., 1997).

Stopped-flow flippase assay

The back-exchange of NBD- and spin-labeled phospholipid analogs from the microsomal membrane to BSA can be observed in a mixture of rat liver microsomes and BSA without separation of BSA from membranes. The quantum yield, and, hence, the fluorescence emission intensity of the NBD group strongly depends on the immediate physicochemical surroundings (Chattopadhyay, 1990). Figure 3 shows the fluorescence emission spectra of P-C6-NBD-PC incorporated into rat liver microsomal membranes (*dashed line*) or bound to BSA (*dotted line*). The extraction of membrane-incorporated NBD-labeled analogs by BSA is accompanied by a significant decrease in NBD fluorescence emission. NBD-labeled analogs that have become bound to BSA are located in a different physicochemical environment than membrane-incorporated NBD-labeled analogs affecting their fluorescence emission (see also Pomorski et al., 1995). The fluorescence emission maximum of the NBD group (λ_{em} = 540 nm, *arrow* in Fig. 3) provides a sensitive measure of those emission changes and allows one to follow the back-exchange of analogs from microsomal membranes.

Figure 4 displays the EPR spectra of SL-PC incorporated into (*A*) rat liver microsomal membranes or (*B*) bound to BSA. Spin-labeled analogs that have become bound by BSA are less mobile than membrane-incorporated analogs. The decreased mobility is reflected in an alteration of the spectral line shape. This alteration, and thus the back-exchange of analogs from membranes to BSA, can be monitored by measuring the amplitude of the low-field peak of the EPR spectrum (*vertical line* in Fig. 4).

We continuously followed the kinetics of back-exchange of NBD- or spin-labeled analogs from rat liver microsomal membranes to BSA by monitoring the changes in NBD fluorescence emission and in EPR spectral line shape, respectively. To this end, we labeled freshly prepared microsomes with NBD- or spin-labeled analogs by preincubation with the analogs for 5 min at room temperature. Subsequently, we mixed the labeled microsomes with a buffered BSA solution in the stopped-flow apparatus (see Materials and Methods). Immediately after mixing (i.e., 10 ms), the NBD fluorescence emission at 540 nm or the low-field peak amplitude of the EPR spectrum was measured as a function of time at room temperature. Both the low-field peak amplitude and the fluorescence emission intensity were found

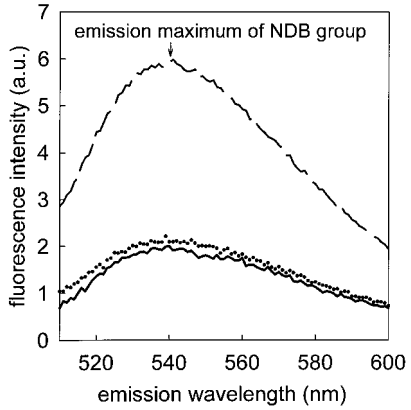

FIGURE 3 BSA completely extracts P-C6-NBD-PC from rat liver microsomal membranes. Fluorescence emission spectrum of a P-C6-NBD-PC/BSA mixture (final concentrations of P-C6-NBD-PC and BSA were 0.2 μM and 1%, respectively) (*dotted line*), compared to the fluorescence emission spectrum that was obtained after incubation of P-C6-NBD-PC-labeled rat liver microsomes (final concentrations of P-C6-NBD-PC and microsomal phospholipids were 0.2 μM and 0.5 mM, respectively) with 1% BSA (final concentration) for 10 min at room temperature (*solid line*). The fluorescence emission spectrum of P-C6-NBD-PC-labeled rat liver microsomes (*dashed line*) is shown as a reference. All fluorescence emission spectra were corrected for the baseline measured in the absence of fluorescent analogs. Spectra were recorded at room temperature.

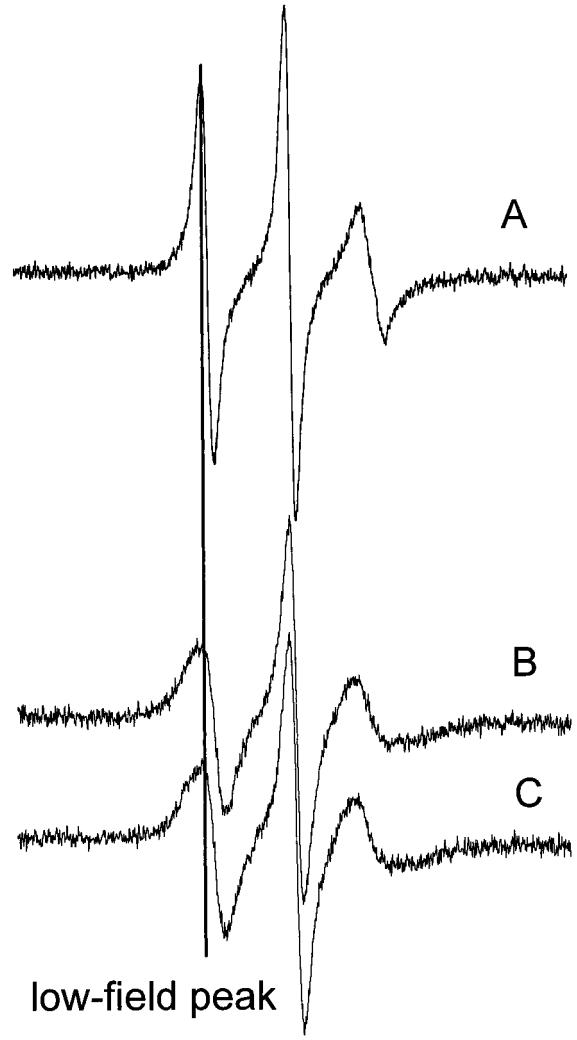

FIGURE 4 BSA completely extracts SL-PC from rat liver microsomal membranes. (*A*) SL-PC incorporated into rat liver microsomal membranes (final concentrations of SL-PC and microsomal phospholipids were 50 μM and 1 mM, respectively). (*B*) EPR spectrum of an SL-PC/BSA mixture (final concentrations of SL-PC and BSA were 50 μM and 5%, respectively). (*C*) Obtained after incubation of SL-PC-labeled rat liver microsomes (final concentrations of SL-PC and microsomal phospholipids were 50 μM and 1 mM, respectively) with 5% BSA (final concentration) for 10 min at room temperature. The specific parameters for measurement of EPR spectra were: conversion time, 81.92 ms; time constant, 20.48 ms; modulation amplitude, 3 G; sweep width, 100 G. All EPR spectra were recorded at room temperature.

to decay in two well-defined phases as shown for SL-PC (Fig. 5) and P-C6-NBD-PC (Fig. 6). Similar curves were obtained for SL-PE and P-C6-NBD-PE, respectively (not shown).

The fast initial decay of the EPR intensity in Fig. 5 reflects the extraction of SL-PC analogs localized in the outer leaflet of the microsomal membrane at the time of mixing with BSA. The half-time of extraction is <3.5 s (see below). We have previously shown, for various membranes, that the extraction of those analogs from the outer leaflet to BSA is very rapid, with a half-time in the order of <4 s (Marx et al., 1997). The second slower decay of the EPR amplitude in Fig. 5 is caused by back-exchange of SL-PC molecules, which move from the inner to the outer microsomal membrane leaflet in the time course of the experiment. As shown below, a theoretical analysis of this phase reveals a fast transbilayer movement of analogs in the order of about 16 s or even less. We note that the kinetics of EPR amplitude decay did not change upon prolonged incubation of labeled microsomes (results not shown). This argues also for a rapid flip-flop of phospholipid analogs: at the time the stopped-flow experiments were performed (i.e., 5 min after mixing of the analogs with the microsomes) the analogs had already fully equilibrated between both leaflets.

The experiment shown in Fig. 7 *A* strongly supports that a similar explanation holds for the first and second phase of BSA-mediated extraction of P-C6-NBD-PC from microsomal membranes. We added P-C6-NBD-PC to rat liver microsomal membranes at room temperature. At two different time points (100 and 300 s) after P-C6-NBD-PC addition, the labeled rat liver microsomes were mixed with a buffered BSA solution, and the NBD fluorescence emission at 540 nm was monitored as a function of time as described above (Fig. 7 *A*). After 100 s, a rapid decay of the NBD fluorescence emission intensity was observed (*solid line*). After 300 s (*dotted line*), a similar rapid initial decay was observed. However, this was followed by a slower decay as seen in Fig. 6. Obviously, the P-C6-NBD-PC molecules had

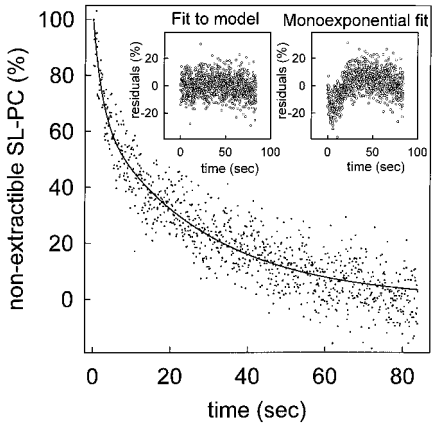

FIGURE 5 Kinetics of the extraction of SL-PC from rat liver microsomal membranes by BSA. Rat liver microsomal membranes were mixed with a dispersion of SL-PC in buffer MB (final concentrations of SL-PC and microsomal phospholipids were 100 μM and 2 mM, respectively) and incubated for 5 min at room temperature. Subsequently, an equal volume of 10% BSA in buffer MB was stopped-flow-mixed with the labeled microsomes and the time course of SL-PC extraction from the microsomal membrane was followed by EPR spectroscopy at room temperature (for details see Materials and Methods). The solid line was obtained by fitting the extraction kinetics to the model shown in Fig. 8. (*Insets*) On the left, the residuals for a fit of the data to the model, and on the right, the residuals for a monoexponential fit of the extraction kinetics are displayed. The specific parameters of EPR measurement were: conversion time, 81.92 ms; time constant, 20.48 ms; modulation amplitude, 3 G.

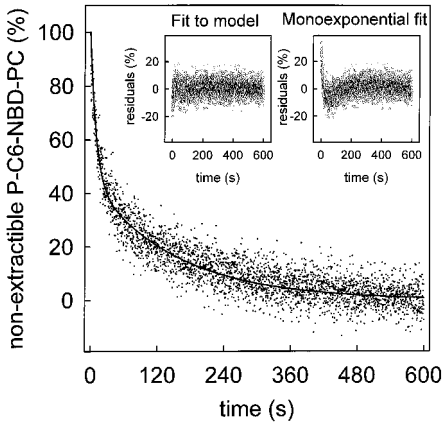

FIGURE 6 Kinetics of the extraction of P-C6-NBD-PC from rat liver microsomal membranes by BSA. Rat liver microsomal membranes were mixed with a dispersion of P-C6-NBD-PC in buffer MB (final concentrations of P-C6-NBD-PC and microsomal phospholipids were 0.4 μM and 1 mM, respectively) and incubated for 5 min at room temperature. Subsequently, an equal volume of 2% BSA in buffer MB was stopped-flow-mixed with labeled microsomes and the time course of P-C6-NBD-PC extraction from the microsomal membrane was followed by fluorescence spectroscopy at room temperature (for details see Materials and Methods). The solid line was obtained by fitting the extraction kinetics to the model shown in Fig. 8. (*Insets*) On the left, the residuals for a fit of the data to the model, and on the right, the residuals for a monoexponential fit of the extraction kinetics are displayed.

entered a protected pool in the microsomal membrane, most plausibly the inner microsomal membrane leaflet. The retardation of the fluorescence emission intensity decay (Fig. 7 *A*, *dotted line*) is the consequence of movement of P-C6-NBD-PC molecules from the inner to the outer microsomal membrane leaflet and their subsequent extraction by BSA. After 100 s, only a minor fraction of analogs moved to the inner leaflet. Therefore, a slow phase of intensity decay cannot be detected. However, after 300 s, a significant amount of analogs was localized on the inner leaflet. This suggests that the half time of analog distribution is between 100 and 300 s (see below).

To prove that NBD- and spin-labeled analogs are completely removed from the microsomal membrane by incubation with BSA, we labeled rat liver microsomal membranes with P-C6-NBD-PC (Fig. 3) or SL-PC (Fig. 4). Upon mixing of the labeled microsomal membranes with BSA, the spectra in Fig. 3 (*solid line*) and Fig. 4 (*spectrum C*) were obtained. Because mixing of P-C6-NBD-PC in buffer with BSA (Fig. 3, *dotted line*) and mixing of SL-PC in buffer with BSA (Fig. 4, *spectrum B*) yielded spectra that were identical to the spectra belonging to the BSA/labeled microsomal membrane mixtures (compare Fig. 3, *dotted line* with *solid line* and Fig. 4, *spectrum B* with *spectrum C*), we conclude that NBD- and spin-labeled analogs were completely extracted from rat liver microsomal membranes by BSA. P-C6-NBD-PE and SL-PE were likewise completely removed from the microsomal membrane by incubation with BSA (data not shown). Note that the concentrations of analogs, microsomal lipids, and BSA were identical to those used in stopped-flow experiments (see also legends to Figs. 3 and 4).

Modeling of transbilayer movement of spin- and NBD-labeled analogs in microsomal membranes

To determine the rate and extent of transbilayer movement of NBD- and spin-labeled analogs, we modeled the data displayed in Figs. 5 and 6 using a three-compartment kinetic model (see Fig. 8 and Appendix). Transbilayer movement of analogs was assumed to be bidirectional in accordance with our observation of complete analog removal from microsomal membranes (see also Buton et al., 1996). Inwardly and outwardly directed analog transbilayer movements and analog extraction by BSA from the outer leaflet were modeled as first-order processes.

When we fitted the time course of BSA-mediated extraction of analogs to the kinetic model depicted in Fig. 8, the rate constants for transmembrane movement of spin-labeled analogs were found to be six- to eightfold higher in comparison to those of NBD-labeled analogs (Table 1). The rate constants k_{+2} for extraction of NBD- and spin-labeled analogs from the outer microsomal membrane leaflet differed by only three- to fourfold (Table 1). As expected, due to the excess of BSA, the exchange process described by the rate

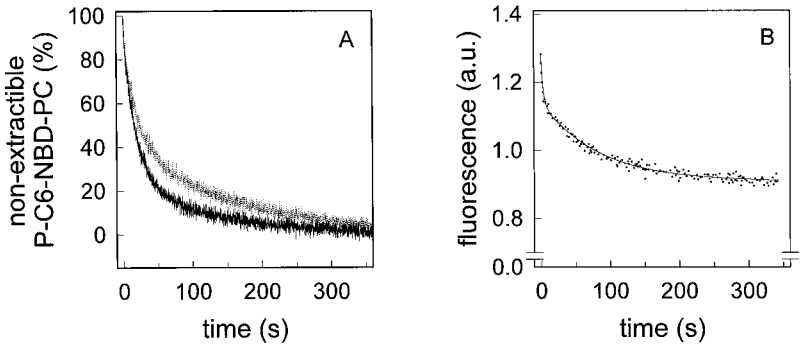

FIGURE 7 (*A*) Evidence for P-C6-NBD-PC and P-C6-NBD-PE redistribution across rat liver microsomal membranes. Microsomal membranes were mixed with a dispersion of P-C6-NBD-PC in buffer MB (final concentrations of P-C6-NBD-PC and microsomal phospholipids were 0.4 μM and 1 mM, respectively) and preincubated for 100 s (*solid line*) and 300 s (*dotted line*), respectively. Subsequently, an equal volume of 2% BSA in buffer MB was stopped-flow-mixed with the preincubated mixtures and the time course of P-C6-NBD-PC extraction from the microsomal membrane was followed by fluorescence spectroscopy at room temperature (for details see Materials and Methods). (*B*) Spontaneous transfer of P-C6-NBD-PE between rat liver microsomes and *N*-Rh-PE-containing acceptor liposomes. Microsomes that had been preincubated with P-C6-NBD-PE for 5 min at room temperature (final concentrations of P-C6-NBD-PE and microsomal phospholipid were 0.2 and 60 μM, respectively) were mixed at time zero with *N*-Rh-PE-containing acceptor liposomes (see Materials and Methods). The sample was stirred continuously and the NBD fluorescence emission intensity (λ_{ex} = 470 nm, λ_{em} = 540 nm) was monitored over time at room temperature. The solid line was obtained by fitting the extraction kinetics to the model shown in Fig. 8. The rate parameters determined for transmembrane motion from this fit to the model were $k_{+1} = 0.0127\ s^{-1}$ and $k_{-1} = 0.0171\ s^{-1}$ and $k_{+2} = 0.3\ s^{-1}$. For $[PL_i]_{t=0}$, a value of 57.3% was deduced from the fit to the model.

constant k_{-2} in Fig. 8 did not contribute to the kinetics. The values that were obtained for k_{-2} by fitting the time course of BSA-mediated extraction of analogs to the kinetic model depicted in Fig. 8 were practically zero. Therefore, we did not include those values in Table 1. For both NBD- and spin-labeled analogs extraction of PC-analogs was faster in comparison to the PE-analog. Although the rate constants were in the same order, PE analogs were found to redistribute across the microsomal membrane significantly faster than the respective PC analogs (*t*-test, $\alpha = 0.05$). The rate constants for inwardly (k_{-1}) and outwardly (k_{+1}) directed transbilayer movement of SL-PC were similar (Table 1). The respective half-times are about 16 s. Although, in the same order, we found significantly higher values of k_{+1} in comparison to k_{-1} for SL-PE (*t*-test, $\alpha = 0.05$). For both NBD-labeled analogs, we found significant differences between the rate constant of inwardly and outwardly directed transbilayer movement. For P-C6-NBD-PC outward movement was faster than the inward movement, whereas the opposite was found for P-C6-NBD-PE. The transbilayer distribution of spin- and NBD-labeled analogs was found to be close to a symmetric one (Table 1). We note a slight preference of both PE analogs for the inner leaflet and of P-C6-NBD-PC for the outer leaflet. The theoretical curves that were calculated using the results of the fit to the three-compartment model and the respective residuals are shown in Figs. 5 and 6. Inspection of the residuals (*insets* in Figs. 5 and 6) indicated no time-dependent deviation of the calculated theoretical curves from the experimental values. However, as indicated by the respective residuals, a monoexponential fit does not provide a satisfying description of the experimental data.

Comparison of the stopped-flow back-exchange technique with previously described continuous assays

To our knowledge, aside from the above-described stopped-flow back-exchange assay, no other assay was described as yet that would allow continuous monitoring of transmembrane redistribution of (short-chain) spin-labeled phospholipid analogs.

Zhang and Nichols (1994) and Hrafnsdottir et al. (1997) showed that transbilayer movement of short-chain NBD-labeled phospholipid analogs can be monitored continuously in biological membranes by taking advantage of the rapid exchange of NBD-labeled analogs between vesicles, which can be followed by fluorescence resonance energy transfer between N-Rh-PE and the NBD-labeled analogs. We applied this assay to rat liver microsomal membranes to get an independent verification for data obtained by the stopped-flow approach. For this purpose, freshly prepared rat liver microsomes were preincubated either with P-C6-NBD-PE or with P-C6-NBD-PC (data not shown) for 5 min at room temperature and, subsequently, *N*-Rh-PE-containing acceptor liposomes were added. Previous studies have demonstrated that *N*-Rh-PE molecules do not transfer between membrane vesicles, whereas P-C6-NBD-phospholipid analog molecules transfer rapidly (Pagano et al., 1981; Nichols and Pagano, 1982). Provided this transfer is much faster in comparison to transbilayer movement of P-C6-NBD-PE, the latter can be determined by the assay. Addition of the acceptor liposomes to P-C6-NBD-PE-preincubated microsomes resulted in depletion of P-C6-NBD-PE from the microsomal membrane by spontaneous transfer to

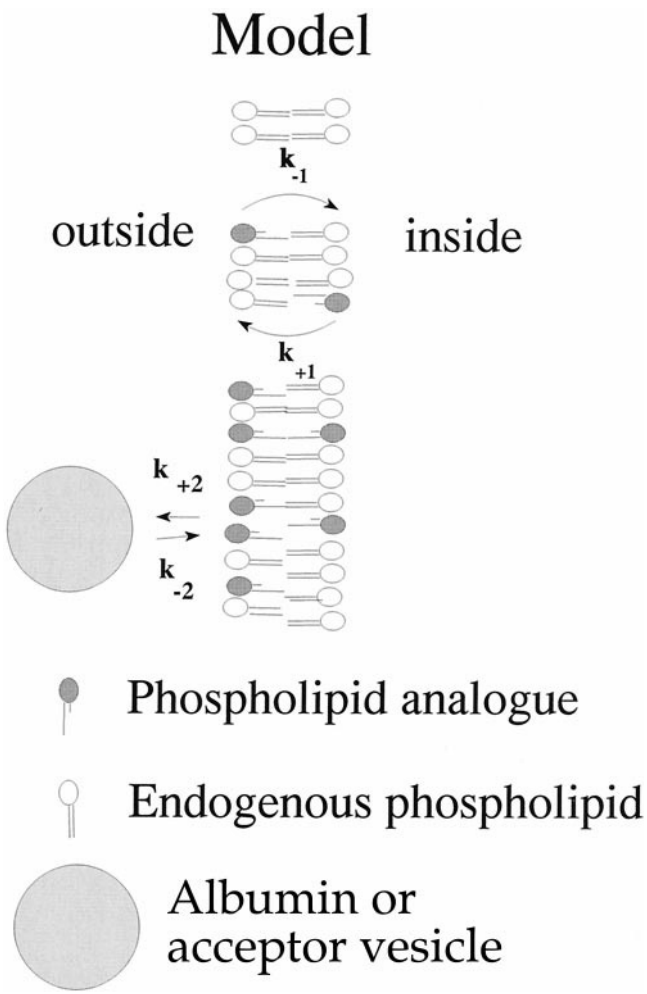

FIGURE 8 Kinetic model describing transfer of phospholipid analogs between microsomes and BSA or between microsomes and *N*-Rh-PE-containing liposomes. k_{+1} and k_{-1} represent the rate constants for outwardly and inwardly directed analog transbilayer movement, respectively. k_{+2} and k_{-2} are the rate constants for analog movement from microsomes to BSA or from microsomes to *N*-Rh-PE-containing acceptor liposomes and vice versa, respectively. The analytical solution for the model is derived in the Appendix.

the acceptor liposomes. The time course of P-C6-NBD-PE transfer from the donor microsomes to the acceptor liposomes could be detected through the decay in NBD fluorescence emission being caused by fluorescence resonance energy transfer from P-C6-NBD-PE to *N*-Rh-PE in the acceptor vesicles (Fig. 7 *B*). The kinetics suggests a biphasic decay. The NBD fluorescence emission decay shown in Fig. 7 *B* is reasonably well fitted by the model (*solid line*). Modeling of our resonance energy transfer data according to the model displayed in Fig. 8 yielded values for the rate constants of inwardly (k_{-1}) and outwardly (k_{+1}) directed analog transbilayer movement (see legend to Fig. 7; not shown for P-C6-NBD-PC) as well as for the steady-state transbilayer distribution, which are in the same order as that found by the stopped-flow back-exchange technique (see Table 1). Consistently, the P-C6-NBD-PE showed a slight preference for the inner leaflet of the microsomal membrane (see legend to Fig. 7).

DISCUSSION

In the present study, we have investigated the transbilayer motion of phospholipids in rat liver microsomal membranes. To this end, we used spin- and NBD-labeled short-chain phospholipid analogs, which have been proven useful for studying transmembrane phospholipid redistribution in subcellular membranes and plasma membranes (Wu and Hubbell, 1993; Gaffet et al., 1995; Angeletti and Nichols, 1998; Gallet et al., 1999). Using such analogs, previous workers could show that phospholipid redistribution in microsomal membranes is both very rapid and mediated by proteins, so-called flippases (Bishop and Bell, 1985; Baker and Dawidowicz, 1987; Herrmann et al., 1990; Buton et al., 1996). However, the molecular nature of those proteins is not known. To identify such flippases and to characterize the underlying mechanism of rapid lipid flip-flop, assays are required that provide a sufficient time resolution for measurement of transbilayer dynamics of phospholipids. Indeed, it became evident from a previous study (Buton et al., 1996) that, due to their comparatively low time resolution, available assays, e.g., the back-exchange assay, may not be able to accurately characterize the transbilayer dynamics of spin-labeled phospholipid analogs in microsomal membranes (see Introduction and below). The transbilayer movement of short-chain NBD-labeled analogs has, to our knowledge, never been investigated in microsomal membranes.

Stopped-flow flippase assay

We developed a stopped-flow back-exchange assay that exploits the fact that the spectral characteristics of membrane-incorporated phospholipid analogs differ from those of BSA-bound analogs. As indicated by the EPR spectrum (Fig. 4), spin-labeled phospholipid analogs bound to BSA experience a higher degree of immobilization than analogs incorporated into a membrane. Moreover they also experience a different physicochemical environment in comparison to (microsomal) membranes, as deduced from the fluorescence emission spectrum of NBD-labeled analogs. Presumably, analogs bound to BSA are exposed to the aqueous phase and, thus, to a more polar environment. Consequently, the quantum yield, and hence the fluorescence emission of NBD-labeled analogs bound to BSA, are significantly lower than those of analogs incorporated into microsomal membranes (see Fig. 3). The kinetics of extraction of spin-labeled analogs by BSA can thus easily be monitored in real time (on-line) by continuously following

TABLE 1 Transbilayer movement and extraction of spin- and NBD-labeled analogs

Analog	k_{+1} (s^{-1})	k_{-1} (s^{-1})	k_{+2} (s^{-1})	$[PL_i]_{t=0}$ (%)
SL-PC	0.043 ± 0.002	0.046 ± 0.001	0.367 ± 0.027	51.9 ± 1.1
SL-PE	0.06 ± 0.011	0.092 ± 0.013	0.201 ± 0.029	61 ± 1.9
P-C6-NBD-PC	0.0071 ± 0.0006	0.0047 ± 0.0004	0.0965 ± 0.0132	40 ± 0.6
P-C6-NBD-PE	0.0086 ± 0.0009	0.0112 ± 0.0006	0.0732 ± 0.0109	56.9 ± 1.6

The data are presented as mean ± standard error ($n = 3$).

k_{+1}, k_{-1}, k_{+2} are defined in Fig. 8. As expected, due to the excess of BSA, the exchange process described by the rate constant k_{-2} in Fig. 8 did not contribute to the kinetics. The values that were obtained for k_{-2} by fitting the experimental data to the model shown in Fig. 8 were practically zero. Therefore, we did not include those values.

$[PL_i]_{t=0}$ is the concentration of analog in the inner leaflet of the microsomal membrane at the time of mixing of the labeled microsomes with BSA.

the alteration in spectral line shape, whereas the kinetics of extraction of NBD-labeled analogs can be determined by following the fluorescence emission of the NBD group. The rapid mixing of labeled membranes with a buffered BSA solution by stopped-flow prevents any delay impeding the detection of rapid transbilayer movement. The delay time due to mixing of the stopped-flow equipment used here is ≤10 ms. This is certainly sufficient to follow transbilayer movement of phospholipid analogs in membranes. The applicability of this approach depends only on the quantitative relation between the rate constants for extraction of analogs by BSA and the rate constants for transbilayer movement of analogs. Only if the extraction step is significantly faster in comparison to the transbilayer movement of analogs, the latter can be characterized by the approach. In that case, we have shown that both the rate constant (or half-time) of transbilayer movement and the transmembrane distribution of analogs can be deduced from fitting of the respective kinetics to a mathematical model (see Figs. 5 and 6).

Phospholipid transbilayer motion in rat liver microsomal membranes is more rapid than previously assumed

The half-times of transbilayer movement determined by EPR stopped-flow for spin-labeled analogs are between 8 to 16 s at room temperature, indicating a very fast flip-flop in rat liver microsomal membranes. The half-times were up to threefold shorter than those determined by Buton et al. (1996) using the same type of analogs. Most likely, this discrepancy can be explained by the limited time resolution of the conventional back-exchange procedure (see above) used by the latter study. For SL-PC, we found no preference for an inward- or outward-directed movement in rat liver microsomes (Table 1) consistent with previous data (Buton et al., 1996). Remarkably, the transbilayer redistribution of the NBD analogs across microsomal membranes was six- to eightfold slower in comparison to the spin-labeled analogs. Apart from those quantitative differences, on a qualitative basis, we observed a similar behavior between the transbilayer dynamics of spin-labeled and fluorescent phospholipids. So, we consistently revealed for both types of labeled analogs a faster redistribution of PE analogs in comparison to the respective PC analogs. Furthermore, we found NBD- and spin-labeled analogs to be close to be equally distributed between both leaflets of the rat liver microsomal membrane. We note a slight preference of PC analogs, at least of P-C6-NBD-PC, to the outer leaflet, whereas, for PE-analogs, the preference was to the inner leaflet. This distribution is in agreement with data on the transmembrane distribution of endogenous phospholipids in rat liver microsomes (Bollen and Higgins, 1980; Higgins and Pigott, 1982).

Suitability of phospholipid analogs for characterization of phospholipid dynamics in microsomal membranes

Recently, it has been shown that similar but radioactively labeled short-chain phospholipid analogs redistribute across rat liver microsomal membranes with a maximum half-time of ~30 s (Buton et al., 1996). Because this half-time is close to the time resolution of the back-exchange assay used in that study, it can therefore only be regarded as an upper limit to the true half-time of redistribution. The true rate of flip-flop of short-chain radioactively labeled analogs is most likely comparable to the rate measured for transbilayer movement of spin-labeled analogs in this study. Consequently, a major influence of the spin group on the kinetics and extent of transbilayer movement of short-chain analogs can be excluded at least as far as rat liver microsomal membranes are concerned. The calculated rate constants for transbilayer movement of spin-labeled analogs were about six- to eightfold higher than those for transbilayer movement of NBD-labeled analogs (Table 1). Thus, we conclude that the reporter moiety may have a significant influence on the kinetics of redistribution of short-chain phospholipid analogs in rat liver microsomal membranes. However, it cannot be ruled out that the truncation of the *sn*-2 acyl chain by itself might alter the behaviour of the analogs relative to endogenous long-chain phospholipids. One may wonder whether endogenous phospholipids with two long fatty acid chains are able to redistribute as rapid as the spin-labeled analogs. Although this is not known for microsomal membranes, it has been shown very recently for vesicles of the

inner membrane of *E. coli* that endogenously newly synthesized PE equilibrates over both membrane leaflets with a half-time of less than one min (Huijbregts et al., 1998). However, even with the particular assay used by Huijbregts et al. (1998), which is only applicable to the phospholipid PE, the kinetics of phospholipid redistribution could not be resolved.

Comparison of the stopped-flow flippase assay with available flippase assays

The novel stopped-flow back-exchange assay circumvents the centrifugation step of the conventional back-exchange assay required for separation of BSA-extracted analogs from membranes (see Introduction). A precondition of the conventional assay is that BSA extracts only those analogs that are located in the outer membrane leaflet at the time of BSA addition. This assumption holds as long as no appreciable transmembrane movement of analogs occurs during the extraction of analogs with BSA. If, as for example in the case of rat liver microsomes, appreciable transmembrane movement of analogs occurs during extraction of analogs with BSA and subsequent centrifugation, the conventional back-exchange assay may yield inaccurate results. This is illustrated in Fig. 9, showing the time course of BSA extraction from rat liver microsomes according to the three-compartment model presented in Fig. 8 and the experimental values obtained for the rate constants of extraction and transbilayer movement of SL-PC (Table 1). It is seen that, due to the rapid transbilayer movement of spin-labeled analogs, a differentiation between analogs on the outer and on the inner leaflet by the conventional back-exchange assay involving a centrifugation step is impossible. Assuming that sample handling, i.e., mixing of membranes with BSA and subsequent centrifugation, can be achieved in as little as 20 s (Buton et al., 1996), a significant part of analogs localized on the inner leaflet at the time of mixing with BSA has already redistributed to the outer leaflet and extracted by BSA.

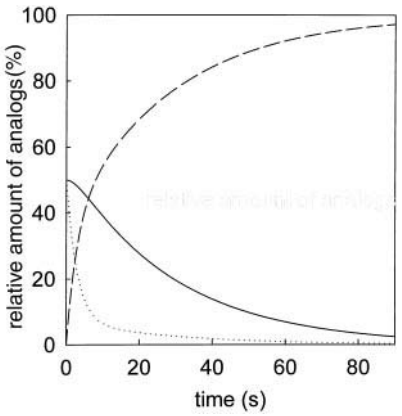

FIGURE 9 Mathematical simulation of the time course of BSA-mediated extraction of spin-labeled phospholipid analogs from microsomal membranes. Simulation is based on the model displayed in Fig. 8. Values for the respective parameters in the model correspond from fitting of experimental curves (see Results and Fig. 5). Time zero corresponds to the addition of BSA to microsomal membranes containing analogs in both membrane leaflets. At time zero, half of the total membrane-incorporated analogs are located in the inner leaflet. The rate constants for transmembrane movement of analogs and extraction of analogs by BSA are $k_{+1} = k_{-1} = 0.04\ s^{-1}$ and $k_{+2} = 0.3\ s^{-1}$, respectively (k_{-2} = zero). (*dashed line*) The amount of extracted analogs; (*dotted line*) analogs localized in the outer leaflet; (*solid line*) analogs localized in the inner leaflet.

Although for spin-labeled analogs, an assay for continuous measurement of rapid transbilayer movement was not available so far, for short-chain NBD-labeled analogs, an assay based on 1) the rapid exchange of those analogs between donor and acceptor vesicles and on 2) resonance energy transfer to a nonexchangeable fluorescent phospholipid analog (*N*-Rh-PE) has been already successful applied to brush border membranes (Zhang and Nichols, 1994) and bacterial membranes (Hrafnsdottir et al., 1997). Applying this assay to rat liver microsomal membranes, we got quite similar results with respect to transbilayer movement and distribution of NBD-labeled phospholipid analogs as we did with our stopped-flow assay based on BSA.

Other methods to trace the transmembrane migration of analogs are based on reduction of the exterior-facing analogs to diamagnetic hydroxylamine or to nonfluorescent derivatives through the action of ascorbate (spin-labeled analogs: Kornberg and McConnell, 1971) and dithionite (NBD-labeled analogs: McIntyre and Sleight, 1991), respectively. The EPR or fluorescence signal remaining after reduction is due to analogs that are oriented to the inner membrane leaflet. Previously, we have shown that those assays can be optimized to assess analogs on the outer leaflet within a few seconds (Marx et al., 1997; Pomorski et al., 1995) enabling also the following of rapid transbilayer movement even of long-chain analogs. However, a prerequisite is that membranes are impermeable to reducing agents in the time course of the assay. Unfortunately, we were unable to follow reduction of exterior-facing spin-labeled and NBD-labeled analogs under conditions where we could definitely exclude that ascorbate and dithionite did permeate the microsomal membrane and reduce analogs on the inner leaflet (data not shown). This precludes also the use of long-chain lipid analogs.

Biological significance of rapid phospholipid transbilayer motion in the endoplasmic reticulum

Our data are consistent with the assumption of a very rapid redistribution of PC and PE in rat liver microsomal membranes, which was not seen in liposomes consisting solely of lipids extracted from the rat liver ER (Marx, U. and A. Herrmann, unpublished results). The rapid redistribution of PC and PE seems to resemble an important process ensuring appropriate membrane biogenesis of the ER (Bishop and

Bell, 1985; Menon, 1995). In rat liver hepatocytes, the endoplasmic reticulum is one of the major sites of PC and PE biosynthesis (McMurray, 1973). Because enzymatic synthesis of PC and PE is an asymmetric process occurring on the cytosolic face of the ER membrane (Coleman and Bell, 1978), a rapid redistribution of newly synthesized PC and PE is necessary to prevent the expansion of one leaflet of the ER which, according to the bilayer-couple-hypothesis (Sheetz and Singer, 1974), could cause undesirable bending, and, eventually, loss of membrane integrity. Indeed, a rough estimate shows that the transbilayer phospholipid dynamics is sufficient to prevent an expansion of one leaflet with respect to the other one. From the initial rate v_i of redistribution of spin-labeled analogs across the microsomal membrane ($v_i = k_{+1} * q$, with q being the amount of analog on the inner leaflet at equilibrium) it can be estimated that the system can transport about 2.5 mmol phospholipid/($h * g$ microsomal protein). This amount of transported lipid corresponds to about 4.5-fold of the total amount of endogenous phospholipid of rat liver microsomes (0.58 mmol endogenous phospholipid/g microsomal protein) assuming 0.46 mg endogenous phospholipid/mg microsomal protein (see Materials and Methods) and an average molecular weight of phospholipid of 800.

Finally, we would like to emphasize that the stopped-flow back-exchange assay allows monitoring of transmembrane redistribution kinetics on-line, is sensitive to small changes in lipid redistribution, and does not consume large amounts of membrane. Preliminary results indicate that the assay is also applicable to other membrane systems like, e.g., yeast microsomal membranes (Marx, U. and Herrmann, A., unpublished results). Currently, we use the newly developed stopped-flow back-exchange assay in a search for yeast mutants that are defective in lipid translocation across the endoplasmic reticulum membrane.

APPENDIX

To determine the rate constants that characterize transfer of phospholipid analogs between microsomes and BSA (Figs. 5 and 6) and microsomes and *N*-Rh-PE-containing acceptor vesicles (Fig. 7 *B*), and also to estimate the transbilayer distribution of phospholipid analogs in the microsomal membrane, we modeled our data using a three-compartment kinetic model (see Fig. 8).

$[PL_o]$ and $[PL_i]$ are the concentrations of analog in the outer and inner leaflet of the microsomal membrane, respectively. $[PL_{tr}]$ is the concentration of analog transferred to BSA or *N*-Rh-PE-containing acceptor vesicles. k_{+1} and k_{-1} represent the rate constants for analog transbilayer movement from the inner to the outer leaflet of the microsomal membrane and vice versa. Transfer of analogs between microsomes and BSA and between microsomes and *N*-Rh-PE-containing acceptor vesicles is characterized by the rate constants k_{+2} and k_{-2}. At the time of vesicle addition ($t = 0$ s), the transmembrane distribution of analogs is at steady-state, i.e.,

$$\frac{[PL_o]_{t=0}}{[PL_i]_{t=0}} = \frac{k_{+1}}{k_{-1}}. \tag{A1}$$

The concentration of analog transferred to BSA or *N*-Rh-PE-containing acceptor vesicles is taken to be zero at the time of vesicle addition (i.e., $[PL_{tr}]_{t=0} = 0\%$).

The model is represented by the following system of differential equations:

$$\frac{d[PL_i]}{dt} = -k_{+1}[PL_i] + k_{-1}[PL_o], \tag{A2a}$$

$$\frac{d[PL_o]}{dt} = k_{+1}[PL_i] - (k_{-1} + k_{+2})[PL_o] + k_{-2}[PL_{tr}], \tag{A2b}$$

$$\frac{d[PL_{tr}]}{dt} = k_{+2}[PL_o] - k_{-2}[PL_{tr}]. \tag{A2c}$$

The analytical solution of the above equation system was performed as follows. Adding Eqs. A2a, A2b, and A2c, it follows immediately that

$$[PL_{tr}] = C - [PL_i] - [PL_o], \tag{A3a}$$

with

$$C = [PL_i]_{t=0} + [PL_o]_{t=0} + [PL_{tr}]_{t=0}. \tag{A3b}$$

Replacing in Eq. A2b the variable $[PL_{tr}]$ by relation Eq. A3a, one gets the inhomogeneous differential equation,

$$\frac{d[PL_o]}{dt} = (k_{+1} - k_{-2})[PL_i] - (k_{-1} + k_{+2} + k_{-2})[PL_o] + Ck_{-2}. \tag{A4}$$

Eqs. A2a and A4 constitute a closed equation system for the variables $[PL_i]$ and $[PL_o]$. The eigenvalues of the homogeneous subsystem are determined by the condition,

$$\det\begin{bmatrix} -(k_{+1} + \lambda) & k_{-1} \\ k_{+1} - k_{-2} & -(k_{-1} + k_{+2} + k_{-2} + \lambda) \end{bmatrix} = 0, \tag{A5}$$

having the characteristic roots

$$\lambda_1 = \frac{k^*}{2}(\sqrt{1 - r} - 1), \tag{A6a}$$

$$\lambda_2 = -\frac{k^*}{2}(\sqrt{1 - r} + 1), \tag{A6b}$$

with

$$k^* = k_{+1} + k_{-1} + k_{+2} + k_{-2}, \tag{A6c}$$

$$r = \frac{4[k_{+1}(k_{+2} + k_{-2}) + k_{-1}k_{-2}]}{(k^*)^2}. \tag{A6d}$$

The general solution of the homogeneous subsystem can be written in the form,

$$[PL_i] = A_1 e^{(\lambda_1 t)} + A_2 e^{(\lambda_2 t)}, \tag{A7a}$$

$$[PL_o] = B_1 e^{(\lambda_1 t)} + B_2 e^{(\lambda_2 t)}. \tag{A7b}$$

Inserting this formulation into Eqs. A2a and A2b, one arrives at the relations,

$$B_i = f_i A_i \quad (i = 1, 2), \tag{A7c}$$

where

$$f_i = \frac{k_{+1} + \lambda_i}{k_{-1}} \quad (i = 1, 2). \tag{A7d}$$

To find a special solution of the inhomogeneous equation system, we use the method of varying constants considering the coefficients A_i in Eqs. A7a and A7b now as time-dependent functions, i.e., $A_1 = A_1(t)$, $A_2 = A_2(t)$. Insertion into Eqs. A2a and A4 yields the differential equations for A_1 and A_2:

$$e^{(\lambda_1 t)} \frac{dA_1}{dt} + e^{(\lambda_2 t)} \frac{dA_2}{dt} = 0, \tag{A8a}$$

$$f_1 e^{(\lambda_1 t)} \frac{dA_1}{dt} + f_2 e^{(\lambda_2 t)} \frac{dA_2}{dt} = k_{-2} C. \tag{A8b}$$

The equation system consisting of Eqs. A8a and A8b is solved by

$$A_1 = A_1(t = 0) + \frac{k_{-2} C}{\lambda_1 (f_1 - f_2)} (1 - e^{(-\lambda_1 t)}), \tag{A8c}$$

$$A_2 = A_2(t = 0) + \frac{k_{-2} C}{\lambda_2 (f_2 - f_1)} (1 - e^{(-\lambda_2 t)}). \tag{A8d}$$

Hence, the general solution of the equation system consisting of Eqs. A2a and A4 reads:

$$[PL_i] = \left[A_1(t = 0) + \frac{k_{-2} C}{\lambda_1 (f_1 - f_2)} (1 - e^{(-\lambda_1 t)}) \right] e^{(\lambda_1 t)} + \left[A_2(t = 0) + \frac{k_{-2} C}{\lambda_1 (f_2 - f_1)} (1 - e^{(-\lambda_2 t)}) \right] e^{(\lambda_2 t)}, \tag{A9a}$$

$$[PL_o] = f_1 \left[A_1(t = 0) + \frac{k_{-2} C}{\lambda_1 (f_1 - f_2)} (1 - e^{(-\lambda_1 t)}) \right] e^{(\lambda_1 t)} + f_2 \left[A_2(t = 0) + \frac{k_{-2} C}{\lambda_1 (f_2 - f_1)} (1 - e^{(-\lambda_2 t)}) \right] e^{(\lambda_2 t)}, \tag{A9b}$$

$$[PL_{tr}] = C - [PL_i] - [PL_o]. \tag{A9c}$$

The values of $A_1(t = 0)$ and $A_2(t = 0)$ are determined by the initial conditions,

$$A_1(t = 0) = \frac{[PL_o]_{t=0} - f_2 [PL_i]_{t=0}}{f_1 - f_2}, \tag{A10a}$$

$$A_2(t = 0) = \frac{f_1 [PL_i]_{t=0} - [PL_o]_{t=0}}{f_1 - f_2}. \tag{A10b}$$

Eqs. A9a–A9c define the complete solution of the equations system consisting of Eqs. A2a–A2c.

We are very grateful to C. Boucsein, Dr. C. Ohlemeyer, and Dr. M. Synowitz for providing us with fresh rat livers. We thank Prof. Dr. R. Tauber (Humboldt-Universität zu Berlin) for his support in preparation of rat liver microsomes. Mrs. B. Hillebrecht and Mrs. S. Schiller are acknowledged for their technical assistance. We are indebted to Prof. Dr. P. F. Devaux for helpful comments and critical discussion of the results presented in the manuscript.

This work was supported by grants from the Deutsche Forschungsgemeinschaft Mu 1017/1-4 to P.M. and GRK 268/97-1 to A.H. and H.G.H. D.W. is a recipient of a fellowship within the Graduiertenkolleg "Dynamics and Evolution of Cellular and Macromolecular Processes."

REFERENCES

Angeletti, C., and J. W. Nichols. 1998. Dithionite quenching rate measurement of the inside–outside membrane bilayer distribution of 7-nitrobenz-2-oxa-1,3-diazol-4-yl-labelled phospholipids. *Biochemistry.* 37: 15114–15119.

Baker, J. M., and E. A. Dawidowicz. 1987. Reconstitution of a phospholipid flippase from rat liver microsomes. *Nature.* 327:341–343.

Berr, F., P. J. Meier, and B. Stieger. 1993. Evidence for the presence of a phosphatidylcholine translocator in isolated rat liver canalicular plasma membrane vesicles. *J. Biol. Chem.* 268:3976–3979.

Bishop, W. R., and R. M. Bell. 1985. Assembly of the endoplasmic reticulum phospholipid bilayer: the PC transporter. *Cell.* 42:51–60.

Bollen, I. C., and J. A. Higgins. 1980. Phospholipid asymmetry in rough- and smooth-endoplasmic-reticulum membranes of untreated and phenobarbital-treated rat liver. *Biochem. J.* 189:475–480.

Buton, X., G. Morrot, P. Fellmann, and M. Seigneuret. 1996. Ultrafast glycerophospholipid-selective transbilayer motion mediated by a protein in the endoplasmic reticulum membrane. *J. Biol. Chem.* 271:6651–6657.

Chattopadhyay, A. 1990. Chemistry and biology of *N*-(7-nitrobenz-2-oxa-1,3-diazol-4-yl)-labelled lipids: fluorescent probes of biological and model membranes. *Chem. Phys. Lip.* 53:1–15.

Coleman, R., and R. M. Bell. 1978. Evidence that biosynthesis of phosphatidylethanolamine, phosphatidylcholine and triacylglycerol occurs on the cytoplasmic side of microsomal vesicles. *J. Cell. Biol.* 76: 245–253.

Colleau, M., P. Herve, P. Fellmann, and P. F. Devaux. 1991. Transmembrane diffusion of fluorescent phospholipids in human erythrocytes. *Chem. Phys. Lip.* 57:29–37.

Connor, J., K. Gillum, and A. J. Schroit. 1990. Maintenance of lipid asymmetry in red blood cells and ghosts: effect of divalent cations and serum albumin on the transbilayer distribution of phosphatidylserine. *Biochim. Biophys. Acta.* 1025:82–86.

Daum, G. 1985. Lipids of mitochondria. *Biochim. Biophys. Acta.* 822: 1–42.

Fellmann, P., A. Zachowski, and P. F. Devaux. 1994. Synthesis and use of spin-labeled lipids for studies of the transmembrane movement of phospholipids. *In* Methods in Molecular Biology: Biomembrane Protocols. II. Architecture and Function. J. M. Graham, and J. A. Higgins, editors. Humana Press Inc., Totowa, NJ. 27:161–175.

Gaffet, P., N. Bettache, and A. Bienvenue. 1995. Transverse redistribution of phospholipids during human platelet activation: evidence for a vectorial outflux specific to aminophospholipids. *Biochemistry.* 34: 6762–6769.

Gallet, P. F., A. Zachowski, R. Julien, P. Fellmann, P. F. Devaux, and A. Maftah. 1999. Transbilayer movement and distribution of spin-labelled phospholipids in the inner mitochondrial membrane. *Biochim. Biophys. Acta.* 1418:61–70.

Haest, C. W. M., G. Plasa, and B. Deuticke. 1981. Selective removal of lipids from the outer membrane layer of human erythrocytes without hemolysis. Consequences for bilayer stability and cell shape. *Biochim. Biophys. Acta.* 649:701–708.

Herrmann, A., A. Zachowski, and P. F. Devaux. 1990. Protein-mediated phospholipid translocation in the endoplasmic reticulum with a low lipid specificity. *Biochemistry.* 29:2023–2027.

Higgins, J. A., and C. A. Pigott. 1982. Asymmetric distribution of phosphatidylethanolamine in the endoplasmic reticulum demonstrated using trinitrobenzenesulphonic acid as a probe. *Biochim. Biophys. Acta.* 693: 151–158.

Hrafnsdottir, S., J. W. Nichols, and A. K. Menon. 1997. Transbilayer movement of fluorescent phospholipids in *Bacillus megaterium* membrane vesicles. *Biochemistry.* 36:4969–4978.

Huijbregts, R. P. H., A. I. P. M. de Kroon, and B. de Kruijff. 1998. Rapid transmembrane movement of newly synthesized phosphatidylethanolamine across the inner membrane of *Escherichia coli. J. Biol. Chem.* 273:18936–18942.

King, M. D., and D. Marsh. 1987. Head group and chain length dependence of phospholipid self-assembly studied by spin-label electron spin resonance. *Biochemistry*. 26:1224–1231.

Kornberg, R. D., and H. M. McConnell. 1971. Inside–outside transitions of phospholipids in vesicle membranes. *Biochemistry.* 10:1111–1120.

Lassmann, G., L. Thelander, and A. Gräslund. 1992. EPR stopped-flow studies of the reaction of the tyrosyl radical of protein R2 from ribonucleotide reductase with hydroxyurea. *Biochim. Biophys. Res. Commun.* 2:879–887.

Marx, U., G. Lassmann, K. Wimalasena, P. Müller, and A. Herrmann. 1997. Rapid kinetics of insertion and accessibility of spin-labelled phospholipid analogs in lipid membranes: a stopped-flow electron spin paramagnetic resonance approach. *Biophys. J.* 73:1645–1654.

Mayer, L. D., M. J. Hope, and P. R. Cullis. 1986. Vesicles of variable sizes produced by a rapid extrusion procedure. *Biochim. Biophys. Acta.* 856: 161–168.

McIntyre, J. C., and R. G. Sleight. 1991. Fluorescence assay for membrane phospholipid asymmetry. *Biochemistry.* 30:11819–11827.

McMurray, W. C. 1973. Chapter 3 *In* Form and Function of Phospholipids. G. B. Ansell, J. N. Hawthorne, R. M. C. Dawson, editors. Elsevier, Amsterdam. 67–94.

Menon, A. K. 1995. Flippases. *Trends Cell Biol.* 5:355–360.

Morrot, G., P. Herve, A. Zachowski, P. Fellmann, and P. F. Devaux. 1989. Aminophospholipid translocase of human erythrocytes: phospholipid substrate specificity and effect of cholesterol. *Biochemistry.* 28: 3456–3462.

Nichols, J. W., and R. E. Pagano. 1982. Use of resonance energy transfer to study the kinetics of amphiphile transfer between vesicles. *Biochemistry.* 21:1720–1726.

Nichols, J. W. 1985. Thermodynamics and kinetics of phospholipid monomer–vesicle interaction. *Biochemistry.* 24:6390–6398.

Pagano, R. E., O. C. Martin, A. J. Schroit, and D. K. Struck. 1981. Formation of asymmetric phospholipid membranes via spontaneous transfer of fluorescent lipid analogs between vesicle populations. *Biochemistry.* 20:4920–4927.

Pomorski, T., A. Herrmann, B. Zimmermann, A. Zachowski, and P. Müller. 1995. An improved assay for measuring the transverse redistribution of fluorescent phospholipids in plasma membranes. *Chem. Phys. Lip.* 77:139–146.

Sheetz, M. P., and S. J. Singer. 1974. Biological membranes as bilayer couples. A molecular mechanism of drug–erythrocyte interactions. *Proc. Natl. Acad. Sci. USA.* 71:4457–4461.

Tauber, R., I. Schenck, D. Josic, V. Gross, P. C. Heinrich, W. Gerok, and W. Reutter. 1986. Different oligosaccharide processing of the membrane-integrated and secretory form of gp 80 in rat liver. *EMBO J.* 5:2109–2114.

Wu, G., and W. L. Hubbell. 1993. Phospholipid asymmetry and transmembrane diffusion in photoreceptor disc membranes. *Biochemistry.* 32: 879–888.

Zhang, Z., and J. W. Nichols. 1994. Protein-mediated transfer of fluorescent-labeled phospholipids across brush border of rabbit intestine. *Am. J. Physiol. Gastrointest. Liver Physiol.* 267:G80–G86.